THE JOURNAL OF BIOLOGICAL CHEMISTRY VOL. 288, NO. 7, pp. 4704–4714, February 15, 2013

Defective in Mitotic Arrest 1 (Dma1) Ubiquitin Ligase Controls G_1 Cyclin Degradation*[S]

Received for publication, October 10, 2012, and in revised form, December 21, 2012 Published, JBC Papers in Press, December 21, 2012, DOI 10.1074/jbc.M112.426593

Sara Hernández-Ortega[‡1,2], Samuel Bru[‡2], Natalia Ricco[‡], Sara Ramírez[‡], Núria Casals[‡], Javier Jiménez[‡], Marta Isasa[§], Bernat Crosas[§], and Josep Clotet[‡3]

From the [‡]Departament de Ciències Bàsiques, Universitat Internacional de Catalunya, 08017 Barcelona and the [§]Departament de Biologia Cellular, Institut de Biologia Molecular de Barcelona, CSIC, 08028 Barcelona, Spain

Background: Dma ubiquitin ligases control the cell cycle in diverse organisms. In humans, these enzymes act as tumor suppressors that prevent aberrant mitosis.
Results: Dma1 targets the cyclin Pcl1 for destruction.
Conclusion: Dma1 ubiquitin ligase activity controls stability of G_1 cyclins.
Significance: Pcl1 is the second reported substrate for Dma1 enzymes. Uncovering new Dma1 substrates could help to elucidate cellular functions of these enzymes.

Progression through the G_1 phase of the cell cycle is controlled by diverse cyclin-dependent kinases (CDKs) that might be associated to numerous cyclin isoforms. Given such complexity, regulation of cyclin degradation should be crucial for coordinating progression through the cell cycle. In *Saccharomyces cerevisiae*, SCF is the only E3 ligase known to date to be involved in G_1 cyclin degradation. Here, we report the design of a genetic screening that uncovered Dma1 as another E3 ligase that targets G_1 cyclins in yeast. We show that the cyclin Pcl1 is ubiquitinated *in vitro* and *in vivo* by Dma1, and accordingly, is stabilized in *dma1* mutants. We demonstrate that Pcl1 must be phosphorylated by its own CDK to efficiently interact with Dma1 and undergo degradation. A nonphosphorylatable version of Pcl1 accumulates throughout the cell cycle, demonstrating the physiological relevance of the proposed mechanism. Finally, we present evidence that the levels of Pcl1 and Cln2 are independently controlled in response to nutrient availability. This new previously unknown mechanism for G_1 cyclin degradation that we report here could help elucidate the specific roles of the redundant CDK-cyclin complexes in G_1.

In all eukaryotic organisms, progression through the G_1 phase of cell cycle is controlled by diverse cyclin-dependent kinases (CDKs)[4] associated to numerous isoforms of cyclins. In budding yeast, the passage through G_1 is mediated by two CDKs: Cdc28, associated to the cyclins Cln1 and Cln2, and Pho85 associated to Pcl1 and Pcl2. These two sets of cyclins are transcribed at the same moment (named START), by the same transcription factors, and it is assumed to be destroyed by the same ubiquitin ligase system (1).

Pcls-CDK complexes could perform the same redundant functions as Clns complexes. Indeed, a *cln1 cln2 pcl1 pcl2* strain is unviable: it fails to extend a discernible bud, and has a large amorphous shape (2). Moreover, most of the Pho85 substrates involved in G_1 cell cycle progression are also substrates of Cdc28: there is evidence for phosphorylation of Sic1, Swi5, Ash1, Whi5, Rga2, and Clb6 by both Pcl-Pho85 and Cln-Cdc28 (2–7). The question arises as to why cells need Pho85 when Cdc28 alone appears able to execute essential cell cycle functions. Andrews and collaborators (2) have suggested that phosphorylation by Pho85 regulates proteins as Cdc28 does, but under different conditions. For example, in the context of DNA damage, the Pho85-Pcl1 complex is the only one active, and hence, is essential for restarting the cell cycle in G_1 (4). Although, the mechanisms that enable the alternating presence of these cyclins remain unknown, selective ubiquitination and degradation are believed to be involved.

The E3 ubiquitin ligase complexes, anaphase-promoting complex and SCF (Skp1/Cdc53/F-box protein) control the two main cell cycle transitions. The former ubiquitinates Clb cyclins after mitosis (5, 6), and the latter targets Cln1 and Cln2 after G_1 (7). A variety of SCFs exist, each of which has a different F-box protein; in fact, the *Saccharomyces cerevisiae* genome contains at least 17 putative F-box proteins, suggesting that, in eukaryotes, the SCF system could control numerous regulatory processes. Under standard growth conditions (YPD at 30 °C) Cln2 is targeted by the SCF-Grr1 system; the fact that Grr1 also regulates nutrient homeostasis (8) suggests that Grr1 could be the link between nutrient sensing and Cln2 turnover (9). Although Pcls are assumed to be degraded by the same ubiquitin-ligase system, the E3 ligase involved in Pcl1 destruction is unknown.

The specificity of F-box interactions could depend on specific destruction box signals present in their substrates. In this regard, a motif present in the Cln2 sequence has recently been described that enables interaction with Grr1 (10). Moreover, this interaction also depends on previous substrate modifica-

* This work was supported by Spanish Ministry of Science and Innovation Grant BFU 2009–09278, now known as the Ministry of Economy and Competitiveness.
[S] This article contains supplemental data.
[1] Supported by a post-graduate Junior Faculty fellowship from the Universitat Internacional de Catalunya and l'Obra Social la Caixa.
[2] Both authors contributed equally to this work.
[3] To whom correspondence should be addressed. Tel.: 34-935042015; Fax: 34-935042001; E-mail: jclotet@uic.es.
[4] The abbreviations used are: CDK, cyclin-dependent kinase; SCF, Skp1/Cdc53/F box protein; Glu-6-PDH, glucose-6-phosphate dehydrogenase.

tion; for example, the destruction of cyclins usually depends on phosphorylation by its own CDK in specific regions with a high content of Pro, Glu, Ser, and Thr, the so-called *PEST* domains. Indeed, Cln2 mutated at the seven potential Cdc28 phosphorylation sites is highly stabilized and render cells insensitive to nutrient and growth inhibitory signals (11). Hence, it is accepted that the instability of Cln cyclins derives from Cdc28-dependent phosphorylation of the cyclin subunit, which allows the interaction of the SCF-Grr1 in a specific domain of Cln2 (10, 12, 13). A similar model has been proposed for mammalian cells, based on findings reported for G_1 cyclins E and D1 (14–16). This model might also be applied to the other group of G_1 cyclins: the Pcls. However, Pcl1 has neither the Grr1 interaction domain proposed in Cln2, nor any PEST sequence, suggesting that an E3 ligase other than SCF might be involved in Pcl1 targeting.

Yeast contains a high number of E3 ligases, some of which are involved in cell-cycle control. These include Dma1 and Dma2, which belong to a small class of proteins that contain a Forkhead-associated (FHA) domain, as well as a RING domain (for review see Ref. 17), of which there are two in humans: Chfr (CHeckpoint protein with FHA and RING domains, (18) and Rnf8 (19). Chfr is a tumor suppressor protein implicated in the antephase checkpoint (18, 20). During the G_2 phase, Dma1 and Dma2 help control the spindle position checkpoint (21) and Swe1 degradation (22), whereas in G_1, the two genes control G_1 progression in response to nutrients by an unknown mechanism (23). Moreover, Dma1 and Dma2 have been described to have ubiquitin ligase activity *in vitro* (23) although their physiological targets are unknown.

Herein we demonstrate that Pcl1 is targeted *in vitro* and *in vivo* by Dma1, and not by Grr1. We uncovered a possible Dma1 docking site sequence required for Pcl1 degradation. Also, we determined that degradation of Pcl1 requires phosphorylation at specific residues of its sequence by its own CDK. Finally, we present evidence that Pcl1 levels change in response to nutrient source through Dma1. The novel mechanism for G_1 cyclin degradation that we report here could help to elucidate the specific roles of the redundant CDK-cyclin complexes in G_1.

EXPERIMENTAL PROCEDURES

Yeast Strains—The strains used in this study are listed in Table 1.

Plasmids—PCL1-TAP and its derivative *pcl1 2A* (with Thr^{39}-Ala and Ser^{43}-Ala substitutions) were expressed from its own promoter in the centromeric plasmid pRS416. The Pcl1, *pcl1 2A*, *pcl1 4A* (with Ser^{14}-Ala, Thr^{70}-Ala, Ser^{117}-Ala, and Ser^{198}-Ala substitutions), *pcl1 DDD** (with Val^{31}-Asn and Pro^{33}-Asn substitutions), and *pcl1 DDD*Δ (with a gap between amino acids Leu^{29} and Asn^{36}) were cloned in pGEX6P1 to be expressed in *Escherichia coli*, and cloned in pRS416 to be expressed in *S. cerevisiae*. *PHO85* was cloned in pEG-KG multicopy plasmid to be overexpressed under control of the *GAL1* promoter and cloned in pGEX6P1 to be expressed in *E. coli*. *PCL9* and *DMA1* genes were cloned in centromeric plasmids (pRS416 and pRS426, respectively) and expressed from their own promoters. *DMA1* was expressed in *E. coli* from pGEX6P1. pGEX6P1::Sic1 construction was previously described in Ref. 24.

TABLE 1
Yeast strains used in this study

Strain	Background	Genotype	Source
	BY4741	*MATa his3Δ1 leu2Δ 200 met15 Δ 0 ura3 Δ 0*	Euroscarf
	W303-1a	*MATa ura3–52; trp1Δ2 leu2–3,112 his3–11 ade2–1 can1–100*	Euroscarf
	BY4741	*Das1::KanMX*	Euroscarf
	BY4741	*Dia2::KanMX*	Euroscarf
	BY4741	*Mfb1::KanMX*	Euroscarf
	BY4741	*Rad9::KanMX*	Euroscarf
	BY4741	*Rcy1::KanMX*	Euroscarf
	BY4741	*Saf1::KanMX*	Euroscarf
	BY4741	*Ubc4::KanMX*	Euroscarf
	BY4741	*Ubc13::KanMX*	Euroscarf
	BY4730	*Ufo1::KanMX*	Euroscarf
	BY4741	*ydr131c::KanMX*	Euroscarf
	BY4741	*ylr224w::KanMX*	Euroscarf
	BY4741	*ymr258c::KanMX*	Euroscarf
	BY4741	*ydr306c::KanMX*	Euroscarf
	BY4741	*ynl311c::KanMX*	Euroscarf
	BY4741	*ylr352w::KanMX*	Euroscarf
YSH75	BY4741	*grr1::KanMX*	This study
YPC639	BY4741	*dma1::KanMX*	This study
YPC651	BY4741	*dma2::KanMX*	This study
YPC748	BY4741	*dma1::LEU2 dma2::KanMX*	This study
YAM42	BY4741	*pho85::URA3*	This study
YAM78	BY4741	*pho85::LEU2*	This study
YSH87	BY4741	*CLN2-TAP::KanMX*	This study
YSH98	BY4741	*CLN2-TAP::KanMX PCL1-TAP::URA3*	This study
YPC708	BY4741	*DMA1-TAP::HIS3*	Euroscarf
YSH82	BY4741	*PCL1-TAP::HIS3*	Euroscarf
YSH83	BY4741	*PCL1-TAP::HIS3 pho85::URA3*	This study
YSH5	BY4741	*PCL9-TAP::KanMX*	This study
YSH12	BY4741	*PCL9-TAP::KanMX pho85::URA3*	This study
YAN31	W303-1a	*SIC1-MYC::TRP1 CLN2-HA::KanMX::NAT*	Posas lab
YSH119	W303-1a	*SIC1-MYC::TRP1 CLN2-HA::KanMX::NAT PCL1-HA::KAN*	This study

Growth Conditions, Cell Synchronization, and Cytometry Analysis—Cells were grown in either YPD medium (1% yeast extract, 2% peptone, and 2% glucose) or in complete synthetic dextrose (SD) medium (0.67% yeast nitrogen base and 2% glucose) containing amino acids for auxotrophic requirements (15 mg/ml of leucine, 5 mg/ml of histidine, and 10 mg/ml of tryptophan) supplemented with either 2% dextrose or 2% raffinose (when indicated). Galactose induction was accomplished by initial growth in SC plus raffinose, followed by an addition of 2% galactose. α-Factor cell synchronization experiments were carried out as previously described (25). Flow cytometry analysis was performed on yeast cells stained with SYBR Green.

Genetic Screening—19 strains defective in different ubquitination systems (indicated in the Table 1) were transformed with a centromeric plasmid carrying *PCL1-HA* and the levels of Pcl1 from exponential growing cells were analyzed.

Immunoblot Analysis—Proteins were detected using the following primary antibodies: anti-PAP 1:4,000 (Sigma, P1291), anti-GST 1:1,000 (GE Healthcare, 27-4577-01), anti-HA monoclonal antibody 1:100 (a gift from Posas Lab), anti-ubiquitin 1:1,000 (Cell Signaling, 3936), anti-FLAG M2 1:500 (Sigma, F3165), or anti-Glu-6-PDH 1:500 (Sigma, A9521). The secondary antibodies used were: donkey anti-goat HRP, sheep anti-mouse HRP, and goat anti-rabbit HRP, all at 1:25,000 (all from Jackson laboratories). Immunoblots were developed using Luminata Forte Western HRP Substrate (Millipore) and images were taken with GeneSnap (Syngene) and quantified with GeneTools (Syngene).

RNA Isolation and Analysis—Cells were harvested and stored at −80 °C. Total RNA was isolated by hot phenol extraction and quantified spectrophotometrically. 2 mg of total RNA were incubated with DNase and reverse transcribed using Quanta qScript cDNA SuperMix according to the manufacturer's instructions. The cDNA was subjected to RT-PCR on a C1000 thermal cycler CFX96 RT system, and expression was normalized to *CDC28*.

Inhibition of Proteasome—Inhibition of proteasome was performed as described (26).

Protein Stability Assay—The stability of the proteins was essentially determined as in Ref. 27. Cycloheximide (Sigma, C4859) was used at a final concentration of 10 mg/ml.

Co-immunoprecipitation of GST-Pho85 and Dma1-TAP from Yeast Extracts—Yeast cells were grown exponentially for 4 h in SC with 2% raffinose. Gene expression was then induced for 4 h by adding galactose at a final concentration of 2%. Cells were harvested (500 ml, $A_{660} = 1.2$), and resuspended in 5 ml of cold extraction buffer A (50 mM Tris, pH 8, 15 mM EDTA, 15 mM EGTA, and 0.1% Triton X-100) containing protease inhibitors (2 mg/ml of pepstatin, 2 mg/ml of leupeptin, 1 mM PMSF, and 1 mM benzamidine), phosphatase inhibitors (10 mM sodium orthovanadate, 25 mM β-glycerophosphate, 1 mM sodium pyrophosphate, and 10 mM sodium fluoride), and 2 mM DTT. Cells were ruptured with glass beads in the FastPrep-24 (Qbiogene, 6 times for 30 s at speed 5) and lysates were clarified by centrifugation at 4 °C for 1 h at 12,000 × *g* and quantified by the Bradford assay (Bio-Rad Laboratories). 3 mg of crude extracts were incubated for 4 h at 4 °C with 200 μl of glutathione-Sepharose beads (GE Healthcare Life Sciences, 17-0756-05). After washing with buffer A, the proteins bound to the beads were resuspended in 30 μl of SDS-PAGE sample buffer, heated at 95 °C for 5 min, and loaded onto SDS-PAGE gels.

In Vitro Binding Assay—Recombinant versions of GST-Pcl1 were purified as described above. The glutathione-Sepharose beads were incubated with yeast cell extracts at 4 °C for 1 h. Beads were washed with buffer A and evaluated by immunoblot analysis.

In Vitro Ubiquitination Assay—GST-Dma1 protein ubiquitin (Ub) ligase activity assays were carried out essentially as described (23). The E1 enzyme (Uba1) and the E2 complex (HIS_{6x}-Ubc13, HIS_{6x}-Mms2) used were from Boston Biochem. The E2 enzyme Ubc4 was purified in our laboratory as a recombinant protein. The E3 GST-Dma1 and the substrate GST-Pcl1 were also purified as described above and N terminally FLAG-tagged using Ub (Sigma, U5382). The reaction was incubated for 5 h at 37 °C, and the ubiquitinated species were separated on 4–15% SDS-PAGE gradient gels.

In Vivo Ubiquitination Assays—Pcl1 was tagged at the C terminus with HIS_{3x}-HA-ProtA and overexpressed from the GAL1 promoter. Tagged proteins were purified using the protocol described in Ref. 28, under fully denatured conditions.

In Vitro Kinase Assays—Kinase assays were performed as previously described (29). Phosphorylated proteins were detected using the Pro-Q Diamond phosphoprotein gel stain kit (Invitrogen).

Phos-tag Gels—10 to 20 μg of protein from cell extracts were separated in 7% polyacrylamide/SDS gels with 10 mM Phos-tag (Wako, 304-93521) plus 20 mM $MnCl_2$ according to the manufacturer's instructions.

LC-MS/MS Analysis—*In vitro* ubiquitination reactions were performed as described above and reaction products were separated by SDS-PAGE on a 10% gel. Gel regions corresponding to ubiquitinated proteins were excised from the gel, reduced, alkylated, trypsinized, and analyzed using a LTQ-Orbitrap Velos mass spectrometer (Thermo Fisher Scientific, San Jose, CA) coupled to an EasyLC (Thermo Fisher Scientific (Proxeon), Odense, Denmark). Peptides were loaded directly onto the analytical column at 1.5–2 μl/min using a wash volume of 4 to 5 times injection volume and separated by reversed-phase chromatography using a 12-cm column with an inner diameter of 75 μm, packed with 5-μm C18 particles (Nikkyo Technos Co., Ltd., Japan). Chromatographic gradients started at 97% buffer A and 3% buffer B with a flow rate of 300 nl/min, and gradually increased to 93% buffer A and 7% buffer B in 1 min, and to 65% buffer A/35% buffer B in 60 min. After each analysis, the column was washed for 10 min with 10% buffer A/90% buffer B. Buffer A was 0.1% formic acid in water. Buffer B was 80% acetonitrile + 0.1% formic acid in water.

The mass spectrometer was operated in positive ionization mode with nanospray voltage set at 2.2 kV and source temperature at 250 °C. Ultramark 1621 for the FT mass analyzer was used for external calibration prior the analyses. Moreover, an internal calibration was also performed using the background polysiloxane ion signal at m/z 445.1200. The instrument was operated in DDA mode and full MS scans with 1 microscan at a resolution of 60,000 were used over a mass range of m/z 100–2000 with detection in the Orbitrap. Auto gain control was set to $1E^6$, dynamic exclusion (60 s) and charge state filtering disqualifying singly charged peptides was activated. In each cycle of DDA analysis, following each survey scan the top 20 most intense ions with multiple charged ions above a threshold ion count of 5000 were selected for fragmentation at normalized collision energy of 35%. Fragment ion spectra produced via collision-induced dissociation were acquired in the Ion Trap, auto gain control was set to $5e^4$, isolation window of 2.0 m/z, activation time of 0.1 ms, and maximum injection time of 100 ms was used. All data were acquired with Xcalibur software version 2.2.

Data Analysis—Raw MS/MS spectra were interpreted with the Proteome Discoverer (version 1.3.0.339, Thermo Fisher Scientific) software suite for peptide identification using Sequest (version 1.20) as the search engine. The data were searched against an in-house generated database containing the 6 proteins present in the *in vitro* assay (Pcl1, Dma1, Ubc13/Mms2, Uba1, and GST). A precursor ion mass tolerance of 7 ppm was applied and up to three missed cleavage sites for trypsin were allowed. The fragment ion mass tolerance was set to 0.5 Da. Oxidation of methionine, ubiquitination (Gly-Gly) in lysine, and protein acetylation at the N-terminal were defined as variable modification; carbamidomethylation on cysteine was set as fixed modification. All spectra were manually validated.

Statistical Analysis—Data were expressed as mean ± S.D. Statistical significance was determined by Student's test for the difference between two normal groups. $p > 0.05$ was considered significant.

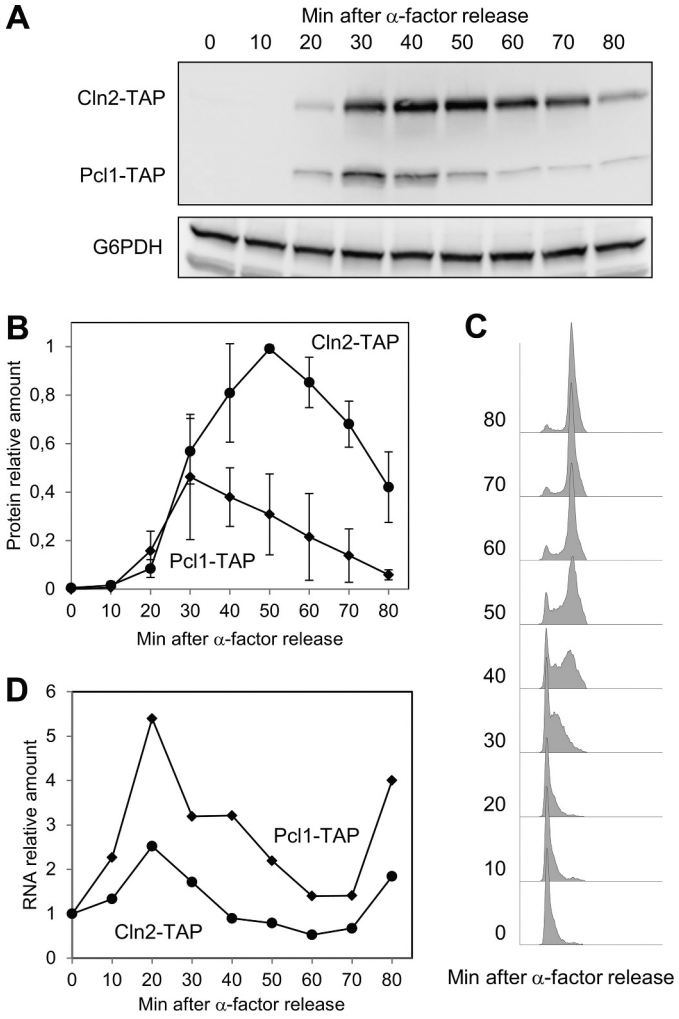

FIGURE 1. **Cln2 and Pcl1 disappear with different kinetics.** Strain YSH98 (double-tagged: *CLN2*-TAP and *PCL1*-TAP) was synchronized at G_1 with α-factor and released in YPD at time 0. Samples were collected at the indicated times and then subjected to several analyses. *A,* Cln2 and Pcl1 protein levels were analyzed by immunoblotting using monoclonal antibodies against TAP-tag; Glu-6-PDH (*G6PDH*) detection was used as a loading control. *B*, quantification of *panel A*. Data ± S.D. from 3 independent experiments are shown. *C,* flow cytometry analysis of DNA content of samples from *panel A*. *D*, RNA levels of Cln2 and Pcl1 of samples from *panel A*. Average from two independent experiments is shown.

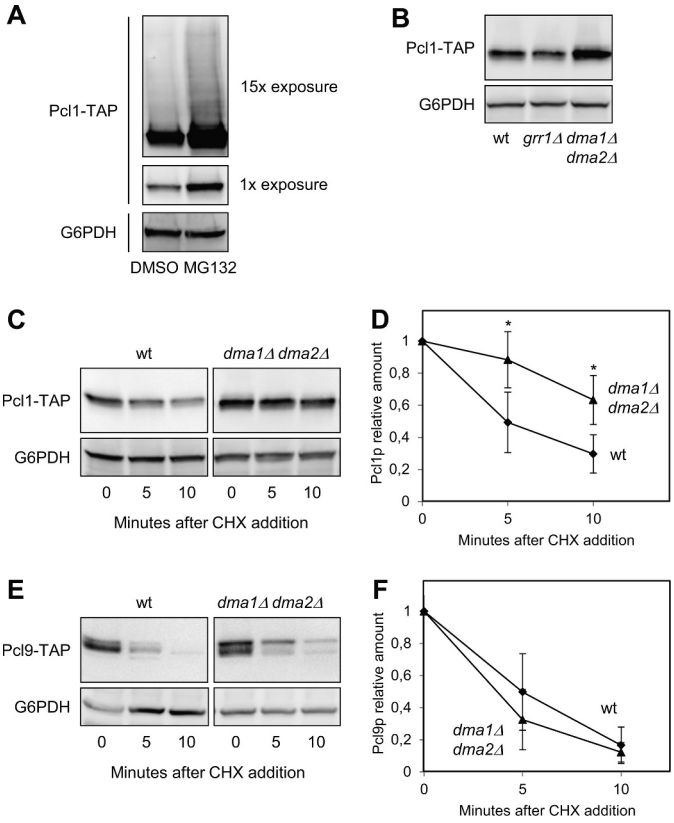

FIGURE 2. **Pcl1 is more stable in the absence of Dma activity.** *A*, Pcl1 levels increased in the presence of proteasomal inhibitors. Cells of strain YSH82 were incubated with either MG132 (a proteasome inhibitor) or a drug vehicle (*DMSO*). 60 min later, samples were taken and Pcl1-TAP protein levels were analyzed by immunoblotting using monoclonal antibodies against TAP-tag. Two different exposures of the immunoblot are shown. As in the rest of the panels, Glu-6-PDH (*G6PDH*) detection was used as a loading control. *B*, relative amounts of Pcl1 in wild type, *grr1*Δ, and *dma1*Δ *dma2*Δ strains. Cells were grown exponentially in rich media, and Pcl1-TAP levels were detected by immunoblotting using monoclonal antibodies. *C,* Pcl1 stability measurements. The indicated strains were grown exponentially in rich media and cycloheximide was added to the medium at time 0. Samples were taken at the indicated times and analyzed for Pcl1-TAP levels by immunoblotting using monoclonal antibodies. *D,* quantification of *panel C*. Data ± S.D. from 3 independent experiments are shown. *, $p > 0.05$ *versus* WT. *E,* Pcl9 stability measurements were carried out as in *panel C*. *F,* quantification of *panel E*. Data ± S.D. from 3 independent experiments are shown.

RESULTS

Turnover of Cln2 and Pcl1 Are Differently Regulated—The G_1 cyclins Cln2 and Pcl1 might act in different physiological situations suggesting that their levels could be differently regulated by uncovered mechanisms. Thus, to elucidate these mechanisms, we examined the levels of the two proteins in a synchronous population of cells as they traversed G_1.

To this end, a double TAP-tagged strain was synchronized in G_1, and then released into the cell cycle. As described, both cyclins appeared simultaneously at 20 min after release (Fig. 1, *A* and *B*), which was 10 min before the cells enter into S phase (Fig. 1*C*). Surprisingly, however, the two cyclins disappeared with different kinetics (Fig. 1*B*), Pcl1 was degraded faster than Cln2. Interestingly, we observed the same result in a strain in which both genes had been tagged with the shorter tag HA, ruling out the possibility that this effect was due to the presence of a specific tag (not shown).

CLN2 and *PCL1* are transcribed simultaneously in G_1 by the same transcription factors and with similar profiles. We confirmed that this was also true under our experimental conditions: both genes show the same expression pattern and peak at 30 min after release (Fig. 1*D*), concluding that differences observed in the levels of the two proteins were probably due to post-transcriptional mechanisms. Thus, our finding suggests that the turnover of each cyclin is regulated differently.

Cln2 and Pcl1 Are Targeted by Different E3 Ligase Systems—Several cyclins are targeted by specific ubiquitination mechanisms and degraded through the proteasome. To test if this is also true with Pcl1, we measured the amount of cyclin in cells treated with the proteasome inhibitor MG132. As shown in Fig. 2*A*, Pcl1 is accumulated in cells whose proteasome had been inhibited. Moreover, under this condition, ubiquitinated proteins are more stable, and normally appear as a "ladder" of slower-moving species on SDS-PAGE. A prominent ladder of this type of Pcl1 species, indicative of ubiquitination, was observed

upon long exposures of Western blots of extracts from cells treated with MG132 (Fig. 2*A*). This observation is consistent with the idea that Pcl1 should be destroyed by ubiquitination targeting and subsequent proteomic degradation. Thus, we decided to search for the ubiquitin ligase involved in such targeting.

Despite the high degree of similarity between Pcl1 and Cln2 at the protein sequence level, Pcl1 lacks the 200 central amino acids of Cln2, which encompass the putative PEST regions as well as a specific domain that promotes ubiquitination by targeting to the E3 ligase Grr1 (10). The absence of this region discards the possibility that Pcl1 was recognized by Grr1. Indeed, whereas the levels of Cln2 are elevated in the *grr1*Δ strain (9), the levels of Pcl1 remain normal (Fig. 2*B*).

To discover the E3-ligase of Pcl1, we transformed a centromeric plasmid carrying *PCL1* to a collection of 18 mutants of different ubiquitination systems, with the aim to find an increase in the amount of cyclin in one of the mutants (see "Experimental Procedures"). This type of screening usually yields small differences, but can help to exclude those strains that do not differ with respect to the amount of Pcl1 in wild type cells. We only observed elevated levels of Pcl1 in two strains: *dia1*Δ and *dma1*Δ *dma2*Δ. Next, we tested the stability of Pcl1 in the *dma1*Δ *dma2*Δ mutant strain by treating cells with cycloheximide. This sort of experiment allows the determination of a protein half-life independently of the initial mRNA levels. In wild type cells, Pcl1 has a half-life of 6.1 ± 0.2 min (Fig. 2*D*), and the same result is observed in the single mutants *dma1*Δ or *dma2*Δ (not shown). However, in the double mutant *dma1*Δ *dma2*Δ, Pcl1 is strongly stabilized (Fig. 2, *C* and *D*).

Finally, we tested whether Dma1 and Dma2 are also involved in control of the stability of Pcl9, a cyclin also present in G_1. As shown in Fig. 2, *E* and *F*, Pcl9 protein has an extremely short half-life (around 4 min) that is not significantly affected by the absence of Dma proteins, suggesting that Dma ubiquitin ligases have a specific effect on Pcl1 stability. Together our findings strongly suggest that Cln2 and Pcl1 are targeted by different E3 ligase systems and that Dma1 and −2 may control G_1 processes by regulating the stability of Pcl1.

Dma1 Interacts with Pcl1 and Targets It for Destruction—We initially tested the possibility that the E3 ligase Dma1 regulates Pcl1 stability through direct targeting by constructing an affinity system based on the expression of Pcl1 in bacteria as a GST fusion protein. Recombinant GST-Pcl1 was then used to bind the Dma1-TAP present in yeast cell extracts. Using this approach, Dma1 was specifically detected via immunoblot analysis of the material retained by the affinity system, indicating that both proteins interact (Fig. 3*A*).

We next checked whether Pcl1-Pho85 complexes interact with Dma1 in yeast cells *in vivo*. As shown in Fig. 3*B*, pull-down of Pho85-GST enables the detection of Dma1, suggesting that Pcl1 and Dma1 proteins also interact *in vivo*.

An *in vitro* autoubiquitination activity of Dma1 and Dma2 has been described (23). We attempted to reconstitute ubiquitination reactions consisting of yeast Uba1, FLAG-tagged Ub, His-tagged E2 enzymes (Msm2 and Ubc13), and full-length GST-Dma1 all purified from *E. coli*. As shown in Fig. 3*C*, this reconstituted system was already able to form long-chain Ub adducts as described (28), indicating that Dma1 was active. Interestingly, when Pcl1 was present, the levels of polyubiquitinated species were far higher, corroborating a Pcl1 ubiquitination that is strictly dependent on the presence of Dma1 associated to Mms2/Ubc13. Ubc4 is another E2 enzyme that promotes Dma1 activity and we wanted to test if such complexes can also ubiquitinate Pcl1. Fig. 3*D* shows that Pcl1 is also ubiquitinated *in vitro* by the Dma1-Ubc4 complexes, although clearly to a lesser extent.

We carried out the same ubiquitination assay, and after 5 h of incubation the reaction mixture was analyzed by mass spectrometry. The spectra clearly showed that some of the ubiquitinated peptides are coming from Pcl1, pointing out residues Lys-82 and Lys-121 as the ones ubiquitinated in our *in vitro* assay (supplemental data). The experiment and posterior mass spectrometry analysis was done in duplicate.

Finally, we decided to check the *in vivo* ubiquitination status of Pcl1. To this end, Pcl1 was double tagged at its endogenous C terminus with a His_6 and TAP epitopes and then purified from denatured lysates using nickel-nitrilotriacetic acid resin (28). Pcl1 ubiquitination levels were determined by immunoblotting for ubiquitin and, to validate that each protein was indeed purified, the TAP epitope also was blotted for analysis. Through this approach, we found that Pcl1 ubiquitination levels were clearly lower in the *dma1*Δ *dma2*Δ strain, indicating that Pcl1 ubiquitination *in vivo* depends on the presence of Dma proteins (Fig. 3*E*). All these results show that Dma1 interacts with Pcl1 and targets it for destruction, a finding that points Pcl1 as the first *bona fide* target of Dma ubiquitin ligases in *S. cerevisiae*.

A Specific Domain Is Necessary for the Dma1-dependent Pcl1 Destabilization—As shown above, Dma1 affects the stability of Pcl1, but not the stability of the very closely related cyclin Pcl9, suggesting that Pcl1 has a region that could facilitate the interaction with Dma1. Alignment of Pcl1 and Pcl9 reveals that the two proteins share a high level of sequence conservation, especially in the N-terminal, except for a short region of 20 amino acids. We wondered whether this region could be a docking site for Dma1. Deletion of amino acids 29 to 36 (a region we called the Dma1 Docking Domain (DDD)) greatly stabilizes Pcl1 *in vivo* (Fig. 4, *A* and *B*), pointing to this region as an important determinant for Dma1 destabilization. Accordingly, the recombinant *pcl1DDD*Δ mutant is less ubiquitinated *in vitro* by Dma1 protein (Fig. 4*C*). It is worth noting that this mutated version of Pcl1 is fully active, as it is still able to allow the phosphorylation of Sic1 (not shown); consequently, we ruled out the possibility that stabilization of the DDD deletion mutant could be due to a general loss of Pcl1 integrity. Also, it is important to stress that the DDD mutants are still phosphorylated by the Pho85 kinase (not shown), excluding the possibility that increased stability comes from the inability to be phosphorylated by the CDK.

High-throughput analyses have revealed proteins associated to Dma1 (30), although the relevance of these interactions remains unknown. Interestingly, several of these proteins contain the DDD motif (including Sid4, a Dma1 substrate in *Schizosaccharomyces pombe* (28)). We performed a ClustalW analysis of the sequence of these proteins, which yielded a consensus sequence for the DDD region: LRVVPS, with the presence of conservative changes in the hydrophobic or charged

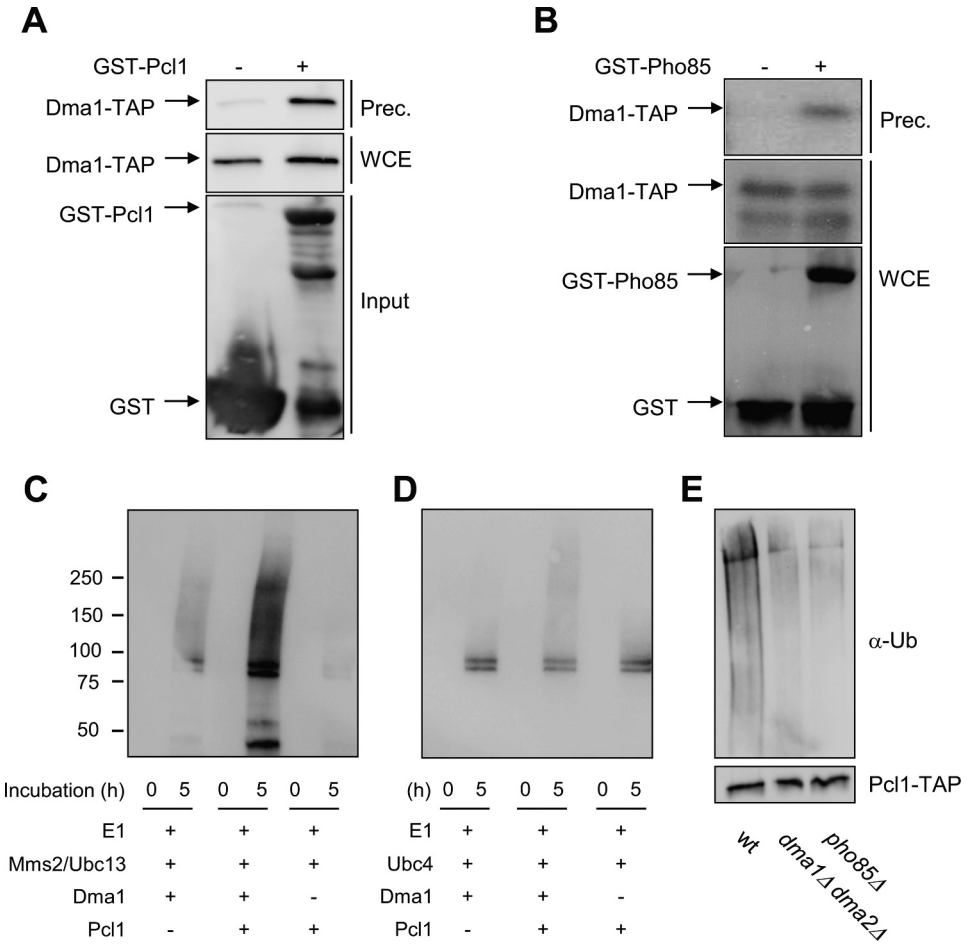

FIGURE 3. **Dma1 interacts and ubiquitinates Pcl1.** *A*, binding *in vitro* assay. Recombinant GST-Pcl1 was purified from *E. coli* and incubated with yeast cell extracts of the strain YPC708 (with a genomic TAP-tagged Dma1) for 45 min, and purified with glutathione-Sepharose beads. Samples were analyzed by immunoblot analysis to detect Dma1-TAP proteins. *WCE,* whole cell extract; *Input*, quantity of Pcl1 used in the trapping. *B*, Pcl1-Pho85 complexes co-immunoprecipitate with Dma1 *in vivo*. Yeast extracts from strains containing untagged *PHO85* or GST-*PHO85* and TAP-tagged *DMA1* (from the chromosomal locus) were precipitated with glutathione-Sepharose beads, and then probed using specific antibodies. *C* and *D,* Pcl1 is ubiquitinated *in vitro* by Dma1. Ubiquitination assays were done by *in vitro* reconstitution of E1-E2-Dma1 complexes (see "Experimental Procedures"). *Panel C* shows Dma1 activity associated to the Mms2-Ubc13 E2 complexes. *Panel D* shows Dma1 activity associated to the Ubc4 E2 enzyme. The reaction was started at time 0 by adding ATP. Samples were taken at 0 and 5 h and analyzed for ubiquitination levels by immunoblotting using α-Ub antibody. *E*, Pcl1 is ubiquitinated *in vivo* in a Dma1-dependent manner. The indicated strains carrying a centromeric plasmid with *PCL1*-His_{6x}-TAP expressed under the *GAL* promoter was grown for 4 h in synthetic complete medium with galactose as a carbon source. The same amount of immunopurified Pcl1-His was separated by SDS-PAGE gels and visualized by immunoblot using an ubiquitin antibody (*top panels*). To validate the levels of Pcl1, the blot was also analyzed using an α-TAP antibody (*bottom panel*).

amino acids (Fig. 4*D*). Interestingly, Cln2 do not have this sequence (Fig. 4*E*), in accordance to the fact that this cyclin is not affected by the presence of Dma1 activity (not shown). To test the importance of such a sequence we changed Pro-5 to Asn, and this substitution strongly stabilized Pcl1 (Fig. 4, *A* and *B*), thereby suggesting that the integrity of DDD is important for the stability of the cyclin. We are currently investigating whether this region could be a true docking domain for Dma1.

Pcl1 Is destabilized by the CDK Pho85—CDK kinases usually phosphorylate their own cyclins, thereby targeting them for destruction, in a negative feedback loop. Hence, we decided to measure Pcl1 protein levels in the absence of Pho85 activity, finding that these levels are six times greater in *pho85*Δ mutants than in wild type cells (Fig. 5*A*). Furthermore, we observed that the half-life of Pcl1 is increased in the absence of Pho85 (Fig. 5, *B* and *C*) to the same extent as Pcl9 (Fig. 5*D*). Accordingly, Pcl1 is less ubiquitinated *in vivo* in the absence of Pho85 activity (Fig. 3*E*). Together these results show that the CDK Pho85 destabilizes Pcl1 probably through a phosphorylation-dependent mechanism.

Pcl1 Is Phosphorylated and Targeted for Destruction by Pho85—We tested this latter possibility by doing *in vitro* phosphorylation experiments using recombinant proteins purified from *E. coli*. Pcl1 has six canonical sites of phosphorylation by Pho85 (Fig. 6*A*) (31). We purified different versions of Pcl1 that carried mutations at these SP/TP sites, and then incubated them with recombinant Pho85 in the presence of ATP. Fig. 6*B* clearly shows that wild type Pcl1 is phosphorylated by Pho85, whereas a mutated version in which Thr^{39} and Ser^{43} are each replaced with an alanine (the *pcl1–2A* version) is markedly less phosphorylated by Pho85. This result does not exclude phosphorylation of other residues, although clearly to a lower extent. Indeed, a Pcl1 that carries a substitution to alanines in the other four SP/TP sites (the *pcl1–4A* version) is phosphorylated to the same extend as wild type Pcl1. This result indicates that Thr^{39} and Ser^{43} of Pcl1 are the major sites phosphorylated by Pho85

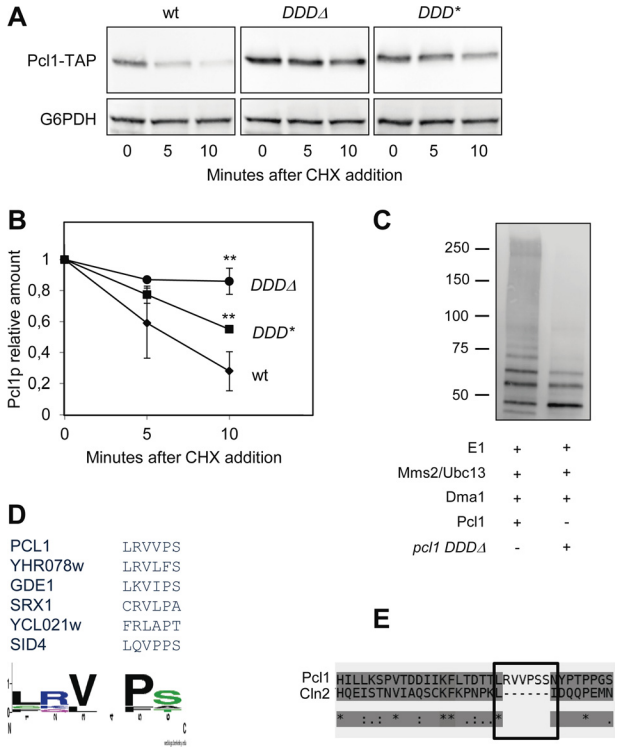

FIGURE 4. **Pcl1 has a putative docking site for Dma1.** *A*, the integrity of the DDD region is essential to maintaining Pcl1 instability *in vivo*. Different alleles of Pcl1 were expressed in wild type cells from a centromeric plasmid under its own promoter: Pcl1 wild type, Pcl1 with a deletion in the DDD region (*DDD*Δ), and Pcl1 with mutations V31N and P33N (*DDD**). All these strains were grown exponentially in rich medium and, at time 0, cycloheximide was added to the medium. Samples were taken at the indicated times and analyzed by immunoblotting using monoclonal antibodies to determine Pcl1-TAP levels. Glu-6-PDH (*G6PDH*) detection was used as a loading control. *B,* quantification of *panel A*. Data ± S.D. from 3 independent experiments are shown. **, $p > 0.01$ *versus* WT. *C, pcl1 DDD*Δ is less ubiquitinated *in vitro* than Pcl1. Ubiquitination assays were done by *in vitro* reconstitution of E1-Mms2-Ubc13-Dma1 complexes (see "Experimental Procedures"). The ubiquitination levels of Pcl1 or *pcl1 DDD*Δ are shown. The reaction was started at time 0 by addition of ATP and finished at 3 h. Samples were taken and analyzed for ubiquitination levels by immunoblotting using α-Ub antibody. *D,* proposed consensus DDD sequence. WebLogo3 analysis (50) of the DDD regions present in several Dma-interacting proteins. *E,* T-Coffee alignment between the N-terminal region of cyclins Pcl1 and Cln2. Cln2 presents a gap that exactly matches the proposed DDD region.

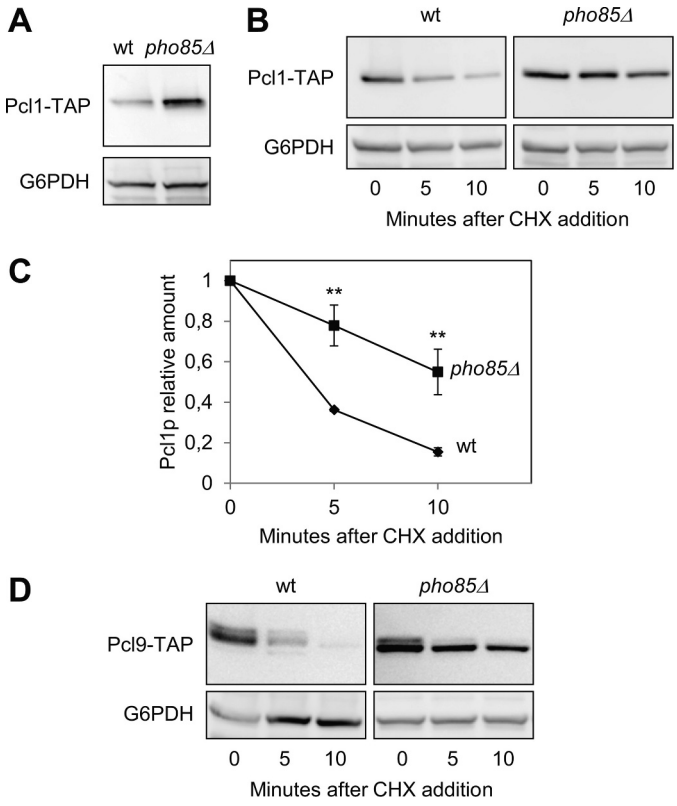

FIGURE 5. **Pcl1 is destabilized by Pho85 activity.** *A*, Pcl1 protein levels are higher in the *pho85*Δ strain. Wild type and *pho85*Δ cells were grown exponentially in YPD, and then Pcl1-TAP levels were determined using immunoblotting with monoclonal antibodies. Glu-6-PDH (*G6PDH*) detection was used as a loading control in each *panel*. *B*, Pcl1 is stabilized in the *pho85*Δ strain. Wild type and *pho85*Δ cells were grown exponentially in rich medium, and cycloheximide was added to the medium at time 0. Samples were taken at the indicated times, and analyzed for Pcl1-TAP levels by immunoblotting using monoclonal antibodies. *C,* quantification of *panel B*. Data ± S.D. from 3 independent experiments are shown. **, $p > 0.01$ *versus* WT. *D,* Pcl9 stability is also controlled by Pho85. Analyses were carried out as in *panel B*.

in vitro. It is interesting to note that these two sites are the nearest to the DDD sequence.

Pcl1 from wild type yeast cells gives a sharp band in standard gel electrophoresis. However, when analyzing extracts in Phos-tag large electrophoresis gels, we distinguished several bands of Pcl1, indicating that such cyclin is phosphorylated *in vivo*. Moreover, the mutant *pcl1–2A* show a clear change in lower mobility bands suggesting that the mutant is phosphorylated to a lesser extent *in vivo* (Fig. 6*C*). More interestingly, the alanine substitution of Thr^{39} and Ser^{43} leads to strong stabilization of Pcl1 (Fig. 6, *D* and *E*), indicating that *in vivo* phosphorylation of Thr^{39} and Ser^{43} is essential for destabilizing the cyclin. As described to other cyclins (10), the substitution of these phosphoacceptor sites by glutamic acid does not mimic the phosphorylation effect and does not decrease the stability of Pcl1 (not shown), suggesting that a negative charge at those two Pcl1 residues is not sufficient for the Dma1 destabilization. Finally, we measured the half-life of the *pcl1–2A* version in a WT and a *dma1*Δ *dma2*Δ strain, and *pcl1–2A* was not further stabilized (Fig. 6*F*), indicating that there was no additive effect between Pho85 and the Ub-ligase.

Pho85 and Dma1 Activities Are Essential for Controlling Pcl1 Levels in the Cell Cycle—At this point, we propose that during G_1, Pcl1 is phosphorylated by Pho85 at the closest residues to the DDD sequence, and that this event increases the ubiquitination of Pcl1 by Dma1 (and probably by Dma2), allowing rapid destruction of the cyclin (see a scheme of the proposed model in Fig. 7*A*). Based on this model, we predicted that cells require both Pho85 and Dma1 activity to down-regulate Pcl1 at the end of G_1. To test this prediction we tracked the levels of Pcl1 from different strains synchronized in G_1 by α factor and subsequently released in rich media. In wild type cells, Pcl1 appears 20 min after release and rapidly disappears, being almost completely depleted at 50 min (Fig. 7*C*). The nonphosphorylatable version of *pcl1–2A* is clearly present for longer periods during the cell cycle (Fig. 7*B*). Similarly, the absence of Dma1/2 proteins also leads to accumulation of Pcl1 beyond the G_1/S transition. The differences observed cannot be explained by differences in the progression through G_1, because the three strains enter into G_2 with the same kinetics (Fig. 7*B*). Thus, we con-

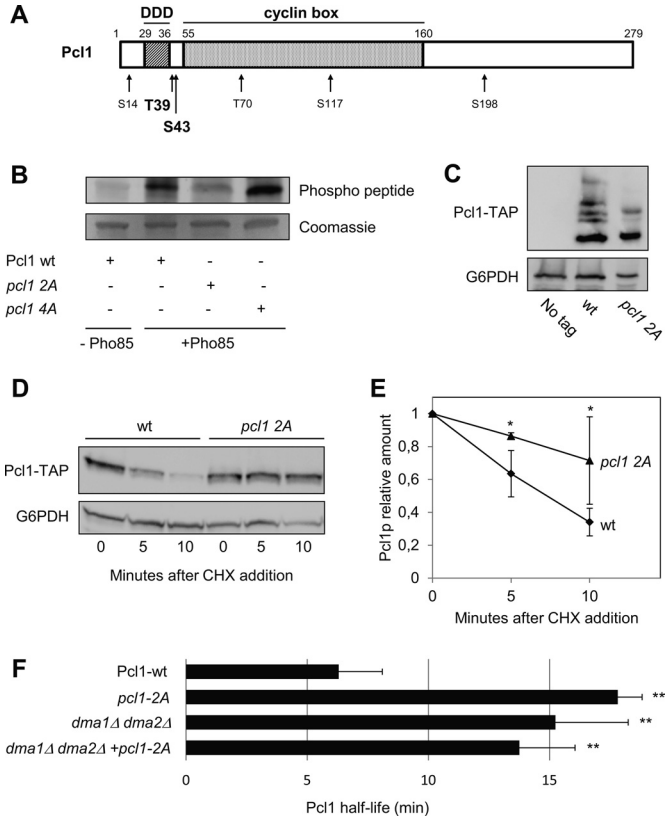

FIGURE 6. **Pcl1 is phosphorylated by Pho85.** *A*, scheme of the Pcl1 protein. *Numbers on top* indicate the amino acid positions. The DDD (Dma1 Docking Domain) region is located between amino acids 29 and 36. *Numbers on bottom* refer to the potential CDK-phosphorylation sites. The proposed Pho85-phosphorylation sites are shown in *bold type* (see below). *B*, Pho85 phosphorylates Pcl1 *in vitro*. Recombinant GST-Pho85 purified from bacteria was incubated with different GST-Pcl1 versions (also purified from bacteria) in the presence of ATP. The 3 Pcl1 versions were: Pcl1 WT, *pcl1 2A* (T39A; S43A), and *pcl1 4A* (S14A; T70A; S117A; S198A). Coomassie staining was used as a loading control. *C*, gel electrophoresis in the presence of 10 mM Phos-tag was carried out to resolve the different phosphorylation populations between Pcl1-TAP and *pcl1 2A*-TAP. Pcl1 levels were analyzed by immunoblotting using monoclonal antibodies. In all panels of the figure, Glu-6-PDH (*G6PDH*) detection was used as a loading control. *D*, nonphosphorylatable versions of Pcl1 are stabilized *in vivo*. Pcl1 WT or *pcl1 2A* were expressed in wild type cells from a centromeric plasmid under its own promoter. Both strains were grown exponentially in rich medium, and cycloheximide was added to the medium at time 0. Samples were taken at the indicated times and analyzed using immunoblotting with monoclonal antibodies to determine Pcl1-TAP levels. *E*, data ± S.D. from 3 independent experiments (performed as in *panel C*) is shown. *, $p > 0.05$ *versus* WT. *F*, Pcl1 half-life is Dma1 and Pho85 dependent. Pcl1-TAP or *pcl1 2A-TAP* were analyzed by Western blot in the noted strains after the addition of cycloheximide (*CHX*). Data ± S.D. from 3 independent experiments are shown. **, $p > 0.01$ *versus* WT.

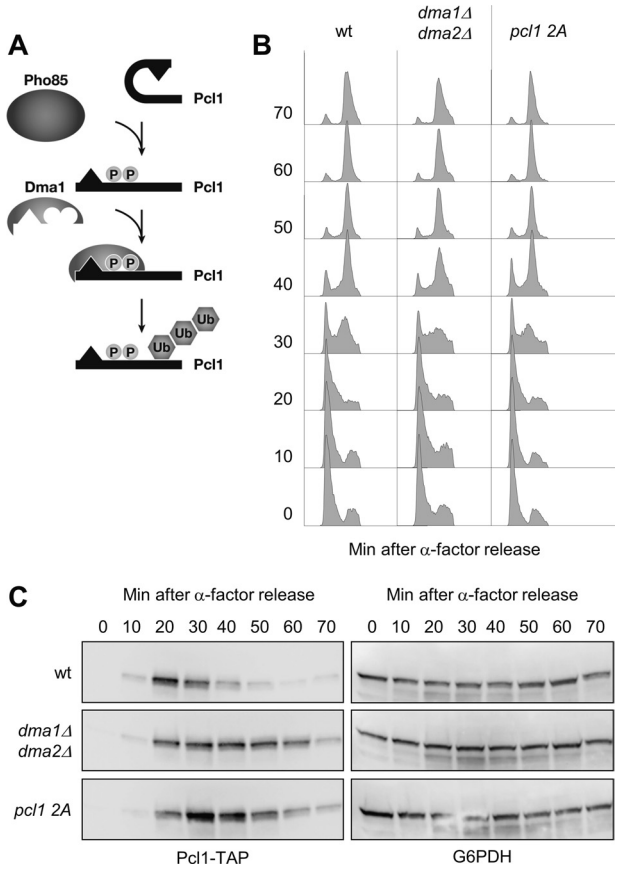

FIGURE 7. **Pho85 and Dma1 activities are essential for controlling Pcl1 levels in the cell cycle.** *A*, proposed model of Pcl1 targeting. Pho85 phosphorylates Pcl1 allowing the recognition by Dma1 that polyubiquitinates and targets Pcl1 for destruction. *B*, the DNA content from cells collected in the experiment shown in *C* was analyzed by flow cytometry at the indicated time points. *C*, Pcl1 requires Dma1 activity to be destabilized under physiological conditions. Wild type cells carrying a Pcl1 or *pcl1 2A* version expressed from a centromeric plasmid and *dma1*Δ *dma2*Δ cells expressing Pcl1, were synchronized with α-factor, and released in rich medium. Samples were collected at the indicated times and then subjected to several analyses. Glu-6-PDH levels were used as a loading control.

cluded that Pho85 and Dma1 are necessary to control Pcl1 levels during the cell cycle.

G_1 Cyclin Levels Are Controlled in Response to Nutrients—An important question arising in this work is: what is the advantage of controlling G_1 cyclins by two different ubiquitination systems? We reasoned that this double control could enable better response to diverse environmental situations. In this regard, Grr1 has been implicated in response to variations in nutrient levels, a finding that links cell cycle control to nutrient availability (9). Dma1 has also been related to nutrient response and G_1 control (32), although the underlying molecular mechanism remains unknown. In this context, we sought to ascertain the behavior of the two cyclins under different nutrient situations.

To this end, we synchronized yeast cells in G_1, released them either in rich media (YPD) or in a synthetic complete media (SD), and then followed the levels of Pcl1 and Cln2. In YPD, Cln2 was more abundant than Pcl1; pointing to the relevance of Cln2 in this growing condition (Fig. 8*A*). However, when the cells are released in SD media, the cyclins seem to have inverted profiles: Pcl1 is more abundant than Cln2. Considering that the two cyclins are transcribed at the same levels under both conditions (not shown), we reasoned that the stability of Cln2 and Pcl1 proteins is differentially affected according to the nutrient status.

It has been predicted that Dma1 levels might be modulated by nutrient conditions (32). Thus, we asked whether the high levels of Pcl1 in SD media could be a consequence of the down-regulation of Dma1 activity. This was indeed the case: Dma1 levels in cells grown in SD were clearly lower than those of cells grown in YPD (Fig. 8*B*). This result indicates that nutrient status regulates levels of Dma ubiquitin ligases, and suggests that physiological control of Pcl1 depends on Dma1 activity. In summary, we propose here that cyclins Pcl1 and Cln2 are degraded by different mechanisms, and that this differential control

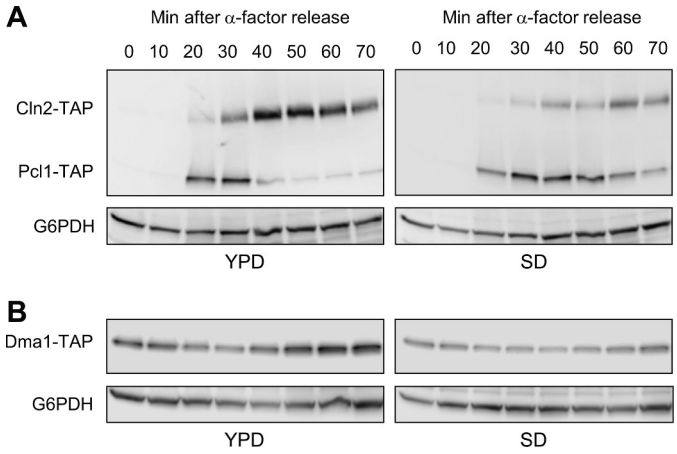

FIGURE 8. **G_1 cyclin levels are controlled in response to nutrients.** *A,* Pcl1 levels are controlled in response to nutrients. The strain YSH98 (double tagged: *CLN2*-TAP and *PCL1*-TAP) was synchronized at G_1 with α-factor. At time 0 the cells were released in either YPD or SD media. Samples were collected at the indicated times, and Cln2 and Pcl1 levels were analyzed by immunoblotting using monoclonal antibodies against TAP-tag. Glu-6-PDH (*G6PDH*) levels were used as a loading control. *B*, Dma1 levels are controlled in response to nutrients. Strain YPC708 was synchronized, sampled, and analyzed as described in *panel A*.

could be essential to ensure correct progression through G_1 in distinct situations of nutrient availability.

DISCUSSION

There are high number of cyclins that control the G_1 phase of eukaryotic cell cycle (33). Such multiplicity is thought to facilitate cellular adaptation to different physiological situations; accordingly, the levels of different cyclins should be differentially regulated. Here we provide substantial evidence that in *S. cerevisiae*, two redundant cyclins expressed at START by the same transcription factors are post-translational regulated by two different E3 ligase systems.

Our motivation for this work came from our earlier observation that Pcl1 is destroyed at the G_1/S boundary, unlike Cln2, which persists until the end of the S phase. Based on this result, we suspected that in *S. cerevisiae* different ubiquitination systems might be involved in destroying distinct G_1 cyclins.

A Novel Function for Dma1: G_1 Cyclin Targeting—The screening designed in this work enabled us to determine the E3 ligases Dia2, and Dma1/2 as controllers of the Pcl1 levels. Interestingly, absence of Dia2 (the name comes from Dig into agar) leads to an invasive growth phenotype (34). It is tempting to speculate that the control of Pcl1, a cyclin involved in morphogenetic events, could be one of the roles of Dia2. Regardless, cycloheximide experiments show that Dia2 activity does not affect Pcl1 stability (not shown), and we propose that the observed effect could be transcriptional. In contrast, we have demonstrated that Dma1 activity does affect Pcl1 stability and that Pcl1 is actually a Dma1 substrate, both *in vitro* and *in vivo*. We think that this result is important for various reasons.

First, the Dma ubiquitin ligases are well conserved across evolution and have been demonstrated to control the cell cycle in diverse organisms: in humans *CHFR* regulates the antephase checkpoint (18); in *S. pombe*, Dma1 controls the SIN, at the end of mitosis (35); and in *S. cerevisiae*, it controls G_2 progression (23). Thus, considering the new G_1 role that we describe here, the Dma ubiquitin ligases can be considered as general cell-cycle regulators.

Second, although Dma enzymes were discovered 10 years ago, Pcl1 is the first *bona fide* substrate of Dma1 described in *S. cerevisiae*. Dma1 also controls Swe1 and Elm1 localization but the mechanism underlying such regulation is unknown and could be an indirect effect (27, 36). Interestingly, Dma1 affects the functionality of septins (21), Swe1, Elm1, and Pcl1, all of these proteins are located at the bud neck, suggesting that the action of the Dma1 is focused mainly at the bud neck.

Different E3 Ligases Control G_1 Cyclin Turnover—The novelty suggested from this work is that the multiplicity of G_1 cyclins is controlled by different E3 ligase systems. To date, SCF was the only E3 involved in the targeting for destruction of several G_1 elements. Indeed, SCF_{Cdc4} is required for degradation of CDK inhibitors Sic1, Far1, Cdc6, and Gcn4 (36–38). Furthermore, SCF_{Grr1} targets cyclins Cln1 and Cln2 (and probably Cln3) for degradation (7, 39). However, our present findings indicate that at least another E3 ubiquitin ligase helps orchestrate G_1 destruction.

The *in vitro* ubiquitination systems reconstituted in our laboratory have shown that Pcl1 is ubiquitinated by Dma1 to a greater extent when it is associated with the Msm2/Ubc13 dimer than when it is associated to Ubc4. The nature of ubiquitin conjugation by E2-E3 complexes is critical because the outcome of ubiquitination is usually determined by the topology of the conjugate. Ubc13-Msm2 is a heterodimeric E2 ligase that forms Lys^{63} chains of polyubiquitin, whereas Ubc4 shows no specificity in ubiquitin lysines and the linkage is usually driven by the ubiquitin ligase (40, 41). Even though Lys^{48}-linked polyubiquitination is the usual signal for directing a protein to proteasomal destruction, Lys^{63}-linked ubiquitin chains have been reported to be involved in some cases of proteasome-dependent degradation (42, 43). Thus, we postulate here that targeting of Pcl1 for degradation by Dma1 may occur via Ubc4 or Msm2/Ubc13.

Specificity of Dma1-Pcl1 Interactions—The specificity of E3 ligase interactions with their substrates probably depends on specific destruction box signals in the latter. In this regard, a short sequence in Cln2 has recently been described as a possible docking site for Grr1 (10). Here we provide preliminary evidence that Dma ubiquitin ligases also might recognize their substrates through a specific sequence, which we have named the DDD. The DDD sequence found in Pcl1 is LRVVPS. However, we must emphasize the fact that, although some amino acids are represented in a greater proportions (see logo of Fig. 4*D*), the DDD region allows for conservative changes in sequence. In the absence of crystallographic data to confirm our hypothesis, we propose here the sequence L(O)V(J)PS(*X*)N as a general DDD sequence (where O represents any charged amino acid, J represents any hydrophobic amino acid, and *X* any amino acid). Interestingly, we searched for this sequence in the yeast proteome and found it in several proteins that control the cell cycle. We are currently investigating if such proteins might be undescribed substrates of Dma1.

Pcl1 Is Phosphorylated and Targeted for Destruction by Its Own CDK—Degradation of Pcl1 after self-catalyzed phosphorylation ensures self-limitation of the activity of the Pho85-Pcl1

complex *in vivo*. This is not a surprising result, given that the cyclins Pcl5 and Pcl9 are destabilized by Pho85 activity (Refs. 45 and 46, and this work), and that Cln1 and Cln2 are also targeted by their own CDK, Cdc28. Thus, our results reinforce the idea that phosphorylation is a general mechanism conserved among the CDKs to control the amount of their own cyclins.

We show that Pcl1 is phosphorylated at Thr^{39} and Ser^{43}. Without excluding other possible residues, we propose that these two residues are the most physiologically relevant to controlling stability of the protein. Indeed, the substitution to alanines of these two residues renders Pcl1 highly stable and, interestingly, the same two residues are found to be the uniquely phosphorylated *in vivo* in a high throughput analysis (44).

The fact that Thr^{39} and Ser^{43} are the two nearest residues to the DDD suggests that this phosphorylation could somehow facilitate interaction between Pcl1 and Dma1. One possibility is that the DDD is usually hidden in Pcl1, but becomes exposed upon phosphorylation of these residues by Pho85, thereby facilitating the interaction between Pcl1 and the E3 ligase. A similar situation has been described in Cln2 that needs a specific region plus the neighboring phosphorylation to be degraded by the Grr1 (10).

Multiplicity in Control, Flexibility in Decisions—The double system of cyclin degradation proposed in this work is probably widespread. For instance, Clb5 and Clb6, which are essential for proper management of S phase, are degraded by anaphase-promoting complex and SCF, respectively (27). Clb5 and Clb6 perform different functions, and accumulation of Clb6 outside of S phase is toxic to cells. However, the G_1 cyclins in *S. cerevisiae* seem to be functionally redundant, which begs the question: are the complexes Cln2-Cdc28 and Pcl1-Pho85 differentially regulated?

Although we cannot definitively answer this question, we have ruminated upon a suggestion that both CDK complexes regulate proteins in the same way but under different conditions (45). This idea is supported by the finding that the G_1 profile of Cln2 and Pcl1 levels depends on nutrient availability. It is striking that Grr1 and Dma1 are also related to the response to changes in nutrient availability (9, 32), and we show here for the first time that Dma1 levels are regulated by nutrient status. Albeit we do not know the mechanism underlying the down-regulation of Dma1, we propose that this process is essential to increase the levels of cyclin Pcl1. Overall, our work supports the notion that the multilayered control of different G_1 CDK-cyclin complexes furnishes cells with the flexibility to adapt to new situations.

A New Conserved Role for Dma1?—Protein sequence alignments between Pcl1 from *S. cerevisiae* and its orthologs from other *Saccharomyces* species indicate that the two putative CDK phosphorylation sites and the DDD sequence are extremely conserved. Moreover, the Pcl1 of *Candida* and other, less related yeasts also contain the DDD region. More interestingly still, is the fact that DDD and the neighboring sequence are conserved in the uncharacterized human cyclin I, which is most similar to Pcl1, and also lacks PEST regions (46). These observations suggest that the destruction of Pcl1 at the G_1/S transition may be conserved through the evolution.

In humans, Dma proteins (named Chfr) play a specific role in the antephase checkpoint. The significance of *CHFR* function in mitosis is reflected by the finding that this E3 ligase is absent or nonfunctional in several transformed cell lines and tumors (47). The study of *CHFR*-null mice presents the *CHFR* as a tumor suppressor that normally acts to prevent aberrant mitosis (48). Although the final target of Chfr is unknown, several lines of evidence support the idea that Cyclin A may be the initial target of the antephase checkpoint (49) thus pointing to the possibility that, in mammals, Chfr would also control cyclin stability. Our laboratory is currently seeking to determine which aspects of the mechanism that we present here are conserved in mammals.

Acknowledgments—We gratefully acknowledge F. Posas for advice and valuable mentoring of J. Clotet all these years. We also gratefully acknowledge S. Menoyo, B. Andrews, and M. Aldea for stimulating discussions, F. Posas for providing yeast strains, M. Pérez for technical assistance, and O. Mirallas for collaboration in some of the experiments. We also thank Armando Terrero for the execution of the scheme shown in Fig. 7A.

REFERENCES

1. Wittenberg, C., and Reed, S. I. (2005) Cell cycle-dependent transcription in yeast. Promoters, transcription factors, and transcriptomes. *Oncogene* **24,** 2746–2755
2. Moffat, J., and Andrews, B. (2004) Late-G_1 cyclin-CDK activity is essential for control of cell morphogenesis in budding yeast. *Nat. Cell Biol.* **6,** 59–66
3. Huang, K., Ferrin-O'Connell, I., Zhang, W., Leonard, G. A., O'Shea, E. K., and Quiocho, F. A. (2007) Structure of the Pho85-Pho80 CDK-cyclin complex of the phosphate-responsive signal transduction pathway. *Mol. Cell.* **28,** 614–623
4. Wysocki, R., Javaheri, A., Kristjansdottir, K., Sha, F., and Kron, S. J. (2006) CDK Pho85 targets CDK inhibitor Sic1 to relieve yeast G_1 checkpoint arrest after DNA damage. *Nat. Struct. Mol. Biol.* **13,** 908–914
5. Irniger, S., and Nasmyth, K. (1997) The anaphase-promoting complex is required in G_1 arrested yeast cells to inhibit B-type cyclin accumulation and to prevent uncontrolled entry into S-phase. *J. Cell Sci.* **110,** 1523–1531
6. Jacobson, M. D., Gray, S., Yuste-Rojas, M., and Cross, F. R. (2000) Testing cyclin specificity in the exit from mitosis. *Mol. Cell. Biol.* **20,** 4483–4493
7. Willems, A. R., Lanker, S., Patton, E. E., Craig, K. L., Nason, T. F., Mathias, N., Kobayashi, R., Wittenberg, C., and Tyers, M. (1996) Cdc53 targets phosphorylated G_1 cyclins for degradation by the ubiquitin proteolytic pathway. *Cell.* **86,** 453–463
8. Benanti, J. A., Cheung, S. K., Brady, M. C., and Toczyski, D. P. (2007) A proteomic screen reveals SCFGrr1 targets that regulate the glycolytic-gluconeogenic switch. *Nat. Cell Biol.* **9,** 1184–1191
9. Barral, Y., Jentsch, S., and Mann, C. (1995) G_1 cyclin turnover and nutrient uptake are controlled by a common pathway in yeast. *Genes Dev.* **9,** 399–409
10. Berset, C., Griac, P., Tempel, R., La Rue, J., Wittenberg, C., and Lanker, S. (2002) Transferable domain in the G_1 cyclin Cln2 sufficient to switch degradation of Sic1 from the E3 ubiquitin ligase SCF(Cdc4) to SCF(Grr1). *Mol. Cell. Biol.* **22,** 4463–4476
11. Lanker, S., Valdivieso, M. H., and Wittenberg, C. (1996) Rapid degradation of the G_1 cyclin Cln2 induced by CDK-dependent phosphorylation. *Science* **271,** 1597–1601
12. Yaglom, J., Linskens, M. H., Sadis, S., Rubin, D. M., Futcher, B., and Finley, D. (1995) p34Cdc28-mediated control of Cln3 cyclin degradation. *Mol. Cell. Biol.* **15,** 731–741
13. Schneider, B. L., Patton, E. E., Lanker, S., Mendenhall, M. D., Wittenberg, C., Futcher, B., and Tyers, M. (1998) Yeast G_1 cyclins are unstable in G_1

phase. *Nature* **395,** 86–89
14. Clurman, B. E., Sheaff, R. J., Thress, K., Groudine, M., and Roberts, J. M. (1996) Turnover of cyclin E by the ubiquitin-proteasome pathway is regulated by cdk2 binding and cyclin phosphorylation. *Genes Dev.* **10,** 1979–1990
15. Diehl, J. A., Zindy, F., and Sherr, C. J. (1997) Inhibition of cyclin D1 phosphorylation on threonine 286 prevents its rapid degradation via the ubiquitin-proteasome pathway. *Genes Dev.* **11,** 957–972
16. Won, K. A., and Reed, S. I. (1996) Activation of cyclin E/CDK2 is coupled to site-specific autophosphorylation and ubiquitin-dependent degradation of cyclin E. *EMBO J.* **15,** 4182–4193
17. Chin, C. F., and Yeong, F. M. (2010) Safeguarding entry into mitosis. The antephase checkpoint. *Mol. Cell. Biol.* **30,** 22–32
18. Scolnick, D. M., and Halazonetis, T. D. (2000) Chfr defines a mitotic stress checkpoint that delays entry into metaphase. *Nature* **406,** 430–435
19. Kolas, N. K., Chapman, J. R., Nakada, S., Ylanko, J., Chahwan, R., Sweeney, F. D., Panier, S., Mendez, M., Wildenhain, J., Thomson, T. M., Pelletier, L., Jackson, S. P., and Durocher, D. (2007) Orchestration of the DNA-damage response by the RNF8 ubiquitin ligase. *Science* **318,** 1637–1640
20. Matsusaka, T., and Pines, J. (2004) Chfr acts with the p38 stress kinases to block entry to mitosis in mammalian cells. *J. Cell Biol.* **166,** 507–516
21. Fraschini, R., Bilotta, D., Lucchini, G., and Piatti, S. (2004) Functional characterization of Dma1 and Dma2, the budding yeast homologues of *Schizosaccharomyces pombe* Dma1 and human Chfr. *Mol. Biol. Cell* **15,** 3796–3810
22. Raspelli, E., Cassani, C., Lucchini, G., and Fraschini, R. (2011) Budding yeast Dma1 and Dma2 participate in regulation of Swe1 levels and localization. *Mol. Biol. Cell* **22,** 2185–2197
23. Loring, G. L., Christensen, K. C., Gerber, S. A., and Brenner, C. (2008) Yeast Chfr homologs retard cell cycle at G1 and G_2/M via Ubc4 and Ubc13/Mms2-dependent ubiquitination. *Cell Cycle* **7,** 96–105
24. Escoté, X., Zapater, M., Clotet, J., and Posas, F. (2004) Hog1 mediates cell-cycle arrest in G_1 phase by the dual targeting of Sic1. *Nat. Cell Biol.* **6,** 997–1002
25. Clotet, J., Escoté, X., Adrover, M. A., Yaakov, G., Garí, E., Aldea, M., de Nadal, E., and Posas, F. (2006) Phosphorylation of Hsl1 by Hog1 leads to a G_2 arrest essential for cell survival at high osmolarity. *EMBO J.* **25,** 2338–2346
26. Liu, C., Apodaca, J., Davis, L. E., and Rao, H. (2007) Proteasome inhibition in wild-type yeast *Saccharomyces cerevisiae* cells. *BioTechniques* **42,** 158–160, 162
27. Jackson, L. P., Reed, S. I., and Haase, S. B. (2006) Distinct mechanisms control the stability of the related S-phase cyclins Clb5 and Clb6. *Mol. Cell. Biol.* **26,** 2456–2466
28. Johnson, A. E., and Gould, K. L. (2011) Dma1 ubiquitinates the SIN scaffold, Sid4, to impede the mitotic localization of Plo1 kinase. *EMBO J.* **30,** 341–354
29. Jeffery, D. A., Springer, M., King, D. S., and O'Shea, E. K. (2001) Multisite phosphorylation of Pho4 by the cyclin-CDK Pho80-Pho85 is semi-processive with site preference. *J. Mol. Biol.* **306,** 997–1010
30. Ho, Y., Gruhler, A., Heilbut, A., Bader, G. D., Moore, L., Adams, S. L., Millar, A., Taylor, P., Bennett, K., Boutilier, K., Yang, L., Wolting, C., Donaldson, I., Schandorff, S., Shewnarane, J., Vo, M., Taggart, J., Goudreault, M., Muskat, B., Alfarano, C., Dewar, D., Lin, Z., Michalickova, K., Willems, A. R., Sassi, H., Nielsen, P. A., Rasmussen, K. J., Andersen, J. R., Johansen, L. E., Hansen, L. H., Jespersen, H., Podtelejnikov, A., Nielsen, E., Crawford, J., Poulsen, V., Sørensen, B. D., Matthiesen, J., Hendrickson, R. C., Gleeson, F., Pawson, T., Moran, M. F., Durocher, D., Mann, M., Hogue, C. W., Figeys, D., and Tyers, M. (2002) Systematic identification of protein complexes in *Saccharomyces cerevisiae* by mass spectrometry. *Nature* **415,** 180–183
31. O'Neill, E. M., Kaffman, A., Jolly, E. R., and O'Shea, E. K. (1996) Regulation of PHO4 nuclear localization by the PHO80-PHO85 cyclin-CDK complex. *Science* **271,** 209–212
32. Bieganowski, P., Shilinski, K., Tsichlis, P. N., and Brenner, C. (2004) Cdc123 and checkpoint forkhead associated with RING proteins control the cell cycle by controlling eIF2γ abundance. *J. Biol. Chem.* **279,** 44656–44666
33. Gopinathan, L., Ratnacaram, C. K., and Kaldis, P. (2011) Established and novel Cdk/cyclin complexes regulating the cell cycle and development. *Results Probl. Cell Differ.* **53,** 365–389
34. Palecek, S. P., Parikh, A. S., and Kron, S. J. (2000) Genetic analysis reveals that FLO11 up-regulation and cell polarization independently regulate invasive growth in *Saccharomyces cerevisiae*. *Genetics* **156,** 1005–1023
35. Guertin, D. A., Venkatram, S., Gould, K. L., and McCollum, D. (2002) Dma1 prevents mitotic exit and cytokinesis by inhibiting the septation initiation network (SIN). *Dev. Cell.* **3,** 779–790
36. Feldman, R. M., Correll, C. C., Kaplan, K. B., and Deshaies, R. J. (1997) A complex of Cdc4p, Skp1p, and Cdc53p/cullin catalyzes ubiquitination of the phosphorylated CDK inhibitor Sic1p. *Cell.* **91,** 221–230
37. Henchoz, S., Chi, Y., Catarin, B., Herskowitz, I., Deshaies, R. J., and Peter, M. (1997) Phosphorylation- and ubiquitin-dependent degradation of the cyclin-dependent kinase inhibitor Far1p in budding yeast. *Genes Dev.* **11,** 3046–3060
38. Drury, L. S., Perkins, G., and Diffley, J. F. (1997) The Cdc4/34/53 pathway targets Cdc6p for proteolysis in budding yeast. *EMBO J.* **16,** 5966–5976
39. Li, W. J., Wang, Y. M., Zheng, X. D., Shi, Q. M., Zhang, T. T., Bai, C., Li, D., Sang, J. L., and Wang, Y. (2006) The F-box protein Grr1 regulates the stability of Ccn1, Cln3, and Hof1 and cell morphogenesis in *Candida albicans*. *Mol. Microbiol.* **62,** 212–226
40. Kim, H. C., and Huibregtse, J. M. (2009) Polyubiquitination by HECT E3s and the determinants of chain type specificity. *Mol. Cell. Biol.* **29,** 3307–3318
41. Rodrigo-Brenni, M. C., Foster, S. A., and Morgan, D. O. (2010) Catalysis of lysine 48-specific ubiquitin chain assembly by residues in E2 and ubiquitin. *Mol. Cell.* **39,** 548–559
42. Kim, H. T., Kim, K. P., Lledias, F., Kisselev, A. F., Scaglione, K. M., Skowyra, D., Gygi, S. P., and Goldberg, A. L. (2007) Certain pairs of ubiquitin-conjugating enzymes (E2s) and ubiquitin-protein ligases (E3s) synthesize nondegradable forked ubiquitin chains containing all possible isopeptide linkages. *J. Biol. Chem.* **282,** 17375–17386
43. Babu, J. R., Geetha, T., and Wooten, M. W. (2005) Sequestosome 1/p62 shuttles polyubiquitinated Tau for proteasomal degradation. *J. Neurochem.* **94,** 192–203
44. Breitkreutz, A., Choi, H., Sharom, J. R., Boucher, L., Neduva, V., Larsen, B., Lin, Z. Y., Breitkreutz, B. J., Stark, C., Liu, G., Ahn, J., Dewar-Darch, D., Reguly, T., Tang, X., Almeida, R., Qin, Z. S., Pawson, T., Gingras, A. C., Nesvizhskii, A. I., and Tyers, M. (2010) A global protein kinase and phosphatase interaction network in yeast. *Science* **328,** 1043–1046
45. Huang, D., Friesen, H., and Andrews, B. (2007) Pho85, a multifunctional cyclin-dependent protein kinase in budding yeast. *Mol. Microbiol.* **66,** 303–314
46. Nakamura, T., Sanokawa, R., Sasaki, Y. F., Ayusawa, D., Oishi, M., and Mori, N. (1995) Cyclin I. A new cyclin encoded by a gene isolated from human brain. *Exp. Cell Res.* **221,** 534–542
47. Sanbhnani, S., and Yeong, F. M. (2012) CHFR. A key checkpoint component implicated in a wide range of cancers. *Cell Mol. Life Sci.* **69,** 1669–1687
48. Yu, X., Minter-Dykhouse, K., Malureanu, L., Zhao, W. M., Zhang, D., Merkle, C. J., Ward, I. M., Saya, H., Fang, G., van Deursen, J., and Chen, J. (2005) Chfr is required for tumor suppression and Aurora A regulation. *Nat. Genet.* **37,** 401–406
49. Geley, S., Kramer, E., Gieffers, C., Gannon, J., Peters, J. M., and Hunt, T. (2001) Anaphase-promoting complex/cyclosome-dependent proteolysis of human cyclin A starts at the beginning of mitosis and is not subject to the spindle assembly checkpoint. *J. Cell Biol.* **153,** 137–148
50. Crooks, G. E., Hon, G., Chandonia, J. M., and Brenner, S. E. (2004) WebLogo. A sequence logo generator. *Genome Res.* **14,** 1188–1190